Monografías Matemáticas *García de Galdeano* **42**, 153–164 (2019)

ANALYSIS OF THE EQUILIBRIA AND LIMIT CYCLE OSCILLATIONS OF FLIGHT DYNAMICS AND AIRFOIL AEROELASTICITY

Sébastien Kolb

Abstract. In aeronautics some phenomena require a nonlinear approach because the linear analysis is not sufficient to catch the underlying physics. Some issues met in the fields of flight dynamics and aeroelasticity are concerned with this feature. This study aims at showing so-called bifurcations implying unpredictable behaviours in the linear frame such as jumps or appearances of limit cycles and thus for which a nonlinear analysis is mandatory in order to catch the real behaviour. The methodology is based on the continuation algorithm amongst others. Practical aspects necessary to perform such an analysis of airplane design are here exposed.

Keywords: bifurcation theory, flight dynamics, aeroelasticity.
AMS classification: 34A34, 34K18, 37G10, 37G15.

Introduction

Some phenomena of aircraft flight dynamics and airfoil aeroelasticity must be examined thanks to a nonlinear approach. In this context, the bifurcation theory allows to set a mathematical frame, to perform an analysis and to understand the underlying dynamics.

As far as the longitudinal flight dynamics of the studied aircraft is concerned, a Hopf bifurcation is diagnosed and gives rise to periodic orbits. Moreover there is a range of elevator deflections δ_e for which there are multiple equilibria. A pitchfork bifurcation seems responsible for this feature leading to a possible stabilization at a nonzero bank angle ϕ. Both situations may surprise the pilot and can be hazardous to manage (especially during a critical phase such as a landing).

The other topic deals with the aeroelasticity of an airfoil whose nonlinear physics come from the pitch stiffness (torsion) or the plunge stiffness (bending) amongst others. Computing the equilibria and the envelope of the periodic orbits (with the continuation algorithm of the *matcont* toolbox of *matlab*) may help investigating some types of nonlinear behaviour.

For example, the plunge stiffness can be hardened $k_h : h \mapsto K_h\left(1 + \xi_h h^2\right)$. The observation of the bifurcation diagrams shows that the Hopf bifurcation associated to a high ξ_h is supercritical whereas the one associated to a low ξ_h is subcritical. This last case may be a dangerous situation since limit cycles may appear before the critical flutter speed determined in the classical linear frame.

In this article, after presenting the employed mathematical framework of dynamical systems, the flight dynamics of the F-18 fighter aircraft is first studied. The modeling of the

flight dynamics and the variables employed are explicited. The phases of longitudinal flight and turn are analysed mathematically then the results are interpreted from the point of view of flight dynamics. Afterwards the nonlinear aeroelasticity of a 2D airfoil section is examined. Two cases of stiffness hardening are examined. The type of the associated Hopf bifurcations is determined and the dangerousness of each situation is assessed.

§1. Mathematical framework and modeling

The models are described under the form of an ordinary differential equation (ODE) whose function $F : \mathbb{R}^n \times \mathbb{R}^p \to \mathbb{R}^n$ (vector field corresponding to the dynamics) is supposed sufficiently regular [5]:

$$\dot{X} = F(X, U) \tag{1}$$

where X is the so-called state vector of dimension n and U is the control vector of dimension p.

Bifurcation theory studies how the structure of the trajectories solution of a dynamical system evolves qualitatively when the control parameters are varying. When limiting the approach to the local bifurcations, then the focus is set on the equilibria, their changes of stability and the apparition of multiple equilibria and limit cycles for certain values of control parameters.

Definition 1. Equilibria are linked to zero dynamics and are the solutions (X, U) of the equation

$$F(X, U) = 0 \tag{2}$$

For most of the equilibria (X_e, U_e) i.e. the non critical ones, the methodology of analysis is based on the theorem of Hartman-Grobman [5] which states that

Theorem 1 (Hartman-Grobman)**.** *If $D_X F(X_e, U_e)$ has no zero or purely imaginary eigenvalues then there is a homeomorphism locally taking orbits of the nonlinear flow to those of the linear flow.*

There are several types of bifurcations which are met in this study i.e. the Hopf bifurcation which is the main one for this issue, the pitchfork bifurcation, the saddle-node bifurcation [5].

Theorem 2 (Hopf)**.** *If $F(X, U) = 0$ has an equilibrium (X_e, U_e) for which $D_X F(X_e, U_e)$ has:*

1. *a pair of purely imaginary eigenvalues $\lambda, \bar{\lambda}$ and no other eigenvalues with zero real parts,*
2. *$\frac{\partial Re\lambda(u)}{\partial u}|_{u_e} \neq 0$ (derivative of the real part of one eigenvalue λ with respect to one control state u of the control vector U),*

then there is a surface of periodic solutions in the center manifold which has a quadratic tangency with the eigenspace of $\lambda(u_e), \bar{\lambda}(u_e)$.

As far as the practical aspects are concerned, the computations will be made with the numerical bifurcation analysis toolbox *matcont* [2]. First the analysis will be focused on the flight dynamics of a fighter aircraft and next on the aeroelasticity of a two-dimensional airfoil.

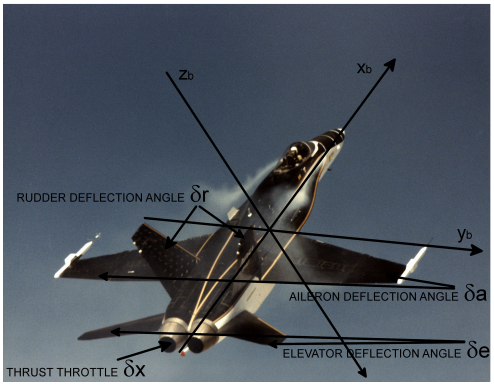

Figure 1: F/A-18 High Alpha Research Vehicle (HARV) flown by NASA's Dryden Flight Research Center, Edwards, CA (`https://www.dfrc.nasa.gov/Gallery/Photo/F-18HARV/Large/EC89-0096-149.jpg`) with added annotations for controls and body-fixed frame

§2. Flight dynamics

The flight dynamics of a F-18 fighter aircraft is studied here. After presenting the model used, two flight phases are studied, that is to say longitudinal flight and turn. Each time, the link is made between the mathematical results and a practical interpretation of the aircraft behaviour.

2.1. Description of the flight dynamics model

The flight dynamics model [4] is taken "as is" that is to say phenomena are observed and analysed but the inner content of the model is not deeply studied.

Concerning the mathematical model, as for the (smooth) function F associated to the dynamical system (1), its expression is polynomial or piecewise polynomial due to the identification of the aerodynamic forces and moments. When studying the whole flight dynamics, the control vector is $U = \{\delta_a, \delta_e, \delta_r, \delta_x\}$ (figure 1 explicits the parts of aircraft especially the tails involved for each control) and the state vector $X = \{\mathcal{M}, \alpha, \beta, p, q, r, \phi, \theta, \psi, x, y, h\}$ contains the variables of airspeed, angles, rotation rates and position (illustrated in figure 2). For a fighter aircraft, the Mach $\mathcal{M}$ which corresponds to the dimensionless ratio of the airspeed to the local speed of sound v_s is often preferred to the classical airspeed V ($\mathcal{M} = V/v_s$).

As far as the pure longitudinal model is concerned, it takes only into account the movement in the vertical plane (no transverse motion), that's why there remain only the state vector $X = \{\mathcal{M}, \alpha, q, \theta, h\}$ and the control vector $U = \{\delta_e, \delta_x\}$ (states presented in the middle of figure 2 and two controls including elevator deflection δ_e of the horizontal tail and thrust throttle δ_x) and besides the other variables are fixed to zero.

The equations of flight dynamics follow the formalism of [4]. The six first ones describe the physics and come from the Newton law (forces and moments), the six last ones are linked to the dynamics of the Euler angles (ϕ, θ, ψ) and of the position components (x, y, h) and

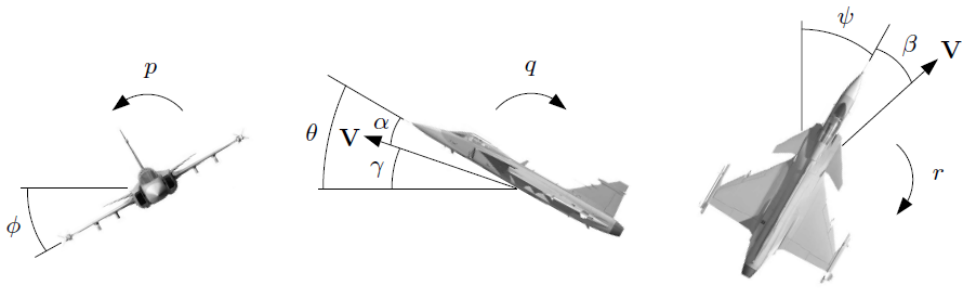

Figure 2: Flight dynamics variables: Euler orientation angles (ϕ, θ, ψ), aerodynamic angles (α, β), angular velocities (p, q, r), flight-path angle γ and airspeed V [6]

traduce some kinematic relations between the variables:

$$
\begin{aligned}
\dot{\mathcal{M}} &= \frac{1}{m v_s}\left[T_m \delta_x \cos\alpha\cos\beta - C_D \frac{1}{2}\rho(v_s\mathcal{M})^2 S - mg\sin\gamma\right] \\
\dot{\alpha} &= q - \frac{1}{\cos\beta}\Bigg[(p\cos\alpha + r\sin\alpha)\sin\beta \\
&\qquad + \frac{1}{m v_s \mathcal{M}}\left(T_m\delta_x\sin\alpha + C_L\frac{1}{2}\rho(v_s\mathcal{M})^2 S - mg\cos\mu\cos\gamma\right)\Bigg] \\
\dot{\beta} &= \frac{1}{m v_s \mathcal{M}}\left[-T_m\delta_x\cos\alpha\sin\beta + C_Y\frac{1}{2}\rho(v_s\mathcal{M})^2 S + mg\sin\mu\cos\gamma\right] \\
\dot{p} &= \frac{I_y - I_z}{I_x} qr + \frac{1}{2I_x}\rho(v_s\mathcal{M})^2 S\, b C_l \\
\dot{q} &= \frac{I_z - I_x}{I_y} pr + \frac{1}{2I_y}\rho(v_s\mathcal{M})^2 S\, c C_m \\
\dot{r} &= \frac{I_x - I_y}{I_z} pq + \frac{1}{2I_z}\rho(v_s\mathcal{M})^2 S\, b C_n \\
\dot{\phi} &= p + q\sin\phi\tan\theta + r\cos\phi\tan\theta \\
\dot{\theta} &= q\cos\phi - r\sin\phi \\
\dot{\psi} &= (q\sin\phi + r\cos\phi)\sec\theta \\
\dot{x} &= v_s\mathcal{M}\cos\gamma\cos\chi \\
\dot{y} &= v_s\mathcal{M}\cos\gamma\sin\chi \\
\dot{h} &= -v_s\mathcal{M}\sin\gamma
\end{aligned}
\tag{3}
$$

The aerodynamic coefficients of drag C_D, side force C_Y, lift C_L, roll moment C_l, pitch moment C_m and yaw moment C_n are piecewise polynomial functions of the angles of attack α, sideslip β and deflection angles of elevator δ_e, aileron δ_a, rudder δ_r and rates of roll p, pitch q and yaw r. More precisely the aerodynamic coefficients are functions of the following variables:

$$C_D(\alpha), C_Y(\beta, \alpha, \delta_r, \delta_a), C_L(\alpha, \delta_e), C_l(\alpha, \beta, p, r, \delta_a, \delta_r), C_m(\alpha, q, \delta_e), C_n(\alpha, \beta, r, \delta_a, \delta_r) \quad (4)$$

In the aforementioned equations (3), χ, γ, μ are the wind axes orientation angles (between the aerodynamic and body frames) whereas ϕ, θ, ψ are the Euler orientation angles (between the body and Earth frames). Moreover the speed of sound v_s and the air density ρ depend on the altitude h. Some data correspond to characteristic dimensions of the aircraft such as the wing span b, the mean aerodynamic chord c, the mass m, the reference area S (wing surface) and the principal moments of inertia I_x, I_y, I_z. Besides the thrust throttle δ_x is here the percentage of maximum available thrust ($T = T_m \delta_x$).

The steps of the analysis methodology are the following ones. The locus of equilibrium points (bifurcation diagram) is first determined. Then the values of critical control parameters (bifurcation values) are calculated and afterwards potentially the locus of bifurcation points. Finally the link is made between the mathematical results (bifurcation theory) and the physical interpretation from the flight dynamics viewpoint. Beneath time simulations are performed so as to illustrate concretely the results of the nonlinear analysis.

2.2. Longitudinal flight

In this section, the longitudinal flight is studied that is to say only the flight in the vertical plane is considered and there are no sideslip and no lateral rotations (for the equilibria of the nominal flight). A classical result of flight dynamics is that for one elevator deflection angle and one thrust throttle position, there is only one (longitudinal) equilibrium. Especially since for a longitudinal equilibrium the sum of the pitching moments must be zero, one elevator deflection δ_e correspond to one angle-of-attack α [8]. But for this F-18 aircraft, several critical behaviours are observed.

2.2.1. Mathematical analysis and numerical results

In order to conduct the analysis, the bifurcation diagram is plotted in figure 3. It presents the angles-of-attack α (equilibria and limit cycles) versus elevator deflection angle δ_e for a thrust throttle fixed at $\delta_x \approx 40\%$. A Hopf bifurcation [5] is diagnosed at $\delta_e \approx -14.9$ deg and creates limit cycles.

Another classical diagram is the locus of bifurcation points presented in figure 4 which shows the critical controls of elevator deflection δ_e and thrust throttle δ_x for which a bifurcation occurs.

There are Hopf bifurcations and branch points. The generalized Hopf bifurcation (where the first Lyapounov coefficient vanishes [2]) at the critical control parameters $\delta_x \approx 53\%, \delta_e \approx -14.3$ deg changes the way periodic orbits are created i.e. for lower or higher elevator deflections than the bifurcation value. The branch points indicates a new phenomenon. Indeed there is a range of elevator deflections ($\delta_e \in [-12\,\text{deg}, -9\,\text{deg}]$, $\delta_x \geq 50\%$) with multiple equilibria (two stable and one unstable). Besides the two distinct curves intersect at a zero Hopf bifurcation (corresponding to a pair of purely imaginary eigenvalues and a zero eigenvalue [2]) at $\delta_x \approx 82\%, \delta_e \approx -11.3$ deg.

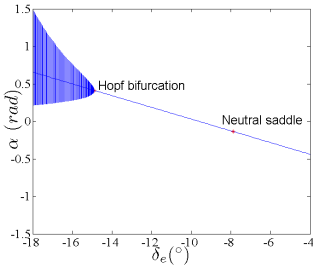

Figure 3: Bifurcation diagram for the longitudinal flight of a F-18 aircraft showing angle-of-attack α in function of elevator deflection angle δ_e

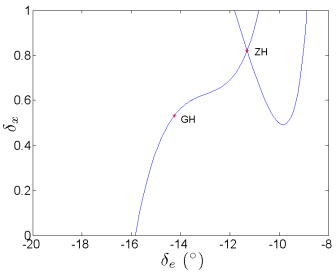

Figure 4: Locus of the bifurcation points for the (δ_e, δ_x) controls

We will next consider the case of a thrust throttle fixed at $\delta_x \approx 70\%$ and study the different bifurcations appearing and especially which physical variables and aircraft mode are involved.

On the one hand, the Hopf bifurcation at the elevator deflection $\delta_e \approx -11.9\,\text{deg}$ involves the variables $(\mathcal{M}, \alpha, q, \theta)$ and is associated to the (pair of complex conjugate) eigenvalues $\lambda_H = \pm 0.298i$. The aircraft begins suddenly to oscillate at a flight path angle of $\gamma = 3.7\,\text{deg}$ after this destabilization. This is a similar phenomenon as the one illustrated figure 3.

On the other hand, the branch point at the elevator deflection $\delta_e \approx -10.9\,\text{deg}$ involves the lateral variables (β, p, r, ϕ) and is associated to the real eigenvalue $\lambda_{BP} = 0$ (the whole model of flight dynamics is exploited for this calculation). That's why from this equilibrium point, it is possible to have stable equilibria with nonzero bank angle ϕ in an asymmetric configuration.

The following time simulations (figures 5 and 6) illustrates both behaviours. Figure 5 shows the behaviour for elevator deflections δ_e higher and lower than the critical Hopf bifurcation value. A stable limit cycle exist for $\delta_e = -13\,\text{deg}$ and a stable equilibrium for $\delta_e = -11.5\,\text{deg}$.

Besides between the two branch point values at elevator deflection angles of $\delta_e = -9.1\,\text{deg}$ and $\delta_e = -10.9\,\text{deg}$, the classical longitudinal equilibrium becomes unstable and the aircraft stabilizes itself at a nonzero bank angle. Figure 6 shows time simulations for an initial bank angle $\phi = -0.3\ rad$ and different elevator deflection angles of $\delta_e = -12\,\text{deg}$ and

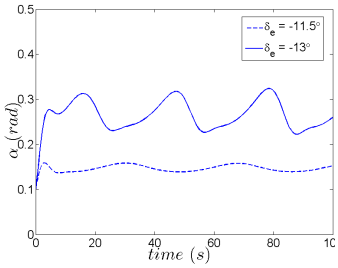

Figure 5: Time simulations for elevator deflection angles δ_e higher and lower than the critical Hopf bifurcation value

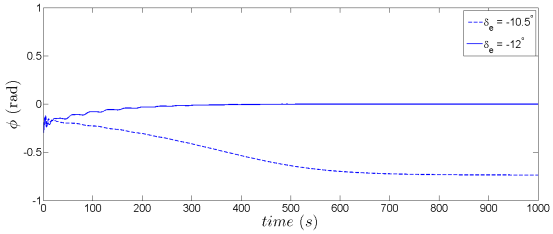

Figure 6: Time simulations for different elevator deflection angles δ_e (between and outside the critical branch point values)

$\delta_e = -10.5$ deg.

Near the bifurcation point, a small change of the elevator deflection angle δ_e can render the classical equilibrium unstable (at a zero bank angle) and leads to a stabilization at a nonzero bank angle ϕ.

Figure 7 is the bifurcation diagram associated to the longitudinal flight. The bank angle ϕ at equilibrium is given in function of the elevator deflection angle δ_e for a throttle $\delta_x \approx 70\%$. In particular, there is a range of elevator deflection angles δ_e with two stable equilibria (nonzero bank angles) and one unstable equilibrium.

Pitchfork bifurcations occur for $\alpha \approx 0.1 rad \approx 5.8$ deg and $\alpha \approx -0.037 rad \approx -2.1$ deg and give rise to several branches of equilibria.

2.2.2. Physical interpretation

In the longitudinal flight dynamics of the F-18 fighter, Hopf bifurcations and pitchfork bifurcations are met. A practical consequence of the existence of a Hopf bifurcation is that the pilot can be astonished by the sudden apparition of peridic orbits during a seemingly normal flight at equilibrium. For example, during a phase with a nonzero flight-path angle γ such as a landing, this sudden change of behaviour can be very hazardous. The loss of stability of the phugoid mode (exchange of airspeed and altitude [8]) seems to be responsible for that.

Moreover there exist also pitchfork bifurcations implying the existence of multiple equilibria for a range of elevator deflection angles δ_e: two stable equilibria with nonzero bank

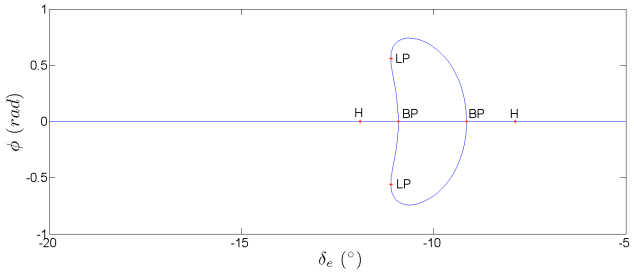

Figure 7: Bifurcation diagram for the longitudinal flight of a F-18 aircraft showing bank angle ϕ in function of the elevator deflection angle δ_e

angle ϕ besides the classical symmetric longitudinal equilibrium (unfortunately unstable). Thus the aircraft can stabilize itself in an unusual asymmetric configuration. Since this motion is very slow and is recoverable by a reverse control action, it seems manageable by a pilot. Nevertheless this propensity of the aircraft to engage itself in a turn due to the loss of stability of the so-called spiral mode [8] may be unpleasant for a pilot.

After analysing the longitudinal flight dynamics and showing some interesting bifurcations and unusual behaviours, the next examined flight phase will be the turn.

2.3. Turn

The effect of aileron deflections on the turn properties (and especially on the roll rate p) are studied here. We will see that it may give rise to nonlinear phenomena and to unexpected behaviour.

The bifurcation diagram is first plotted in figure 8 with the thrust throttle fixed at $\delta_x = 0.5$ and the elevator deflection angle at $\delta_e = -15°$. Limit points (also called fold or saddle-node bifurcation [5]) appear. Theses last ones lead to a jump of roll rate p near the aileron deflections $\delta_a = \pm 32$ deg and is illustrated in the time simulations of figure 9. Nevertheless at an aileron deflections $\delta_a = \pm 18$ deg, the high roll rate may suddenly disappear.

From the physical point of view, at the mechanical limits of the authorized aileron deflection range, the pilot must be careful since the flight dynamics meets some jumps and hysteresis phenomena. The irreversible, quick and unexpected nature of such phenomenona can lead to a hazardous situation with a high roll rate. Thus an advice for the the pilot is to avoid using the ailerons too closely of their mechanical limits.

After examining the flight dynamics of a F-18 fighter aircraft during the phases of longitunal flight and turn thus revealing the existence of diverse types of bifurcations and of unintuitive behaviours, we will next treat the case of nonlinear aeroelasticity of a two-dimensional airfoil.

§3. Airfoil aeroelasticity

After describing the classical model for the aeroelasticity of a 2D airfoil section and its nonlinear terms, the influence of these last ones on the global system behaviour is assessed.

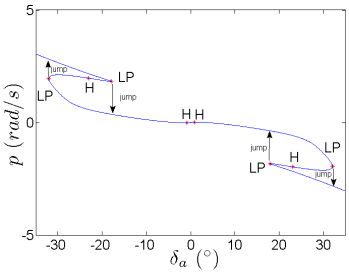

Figure 8: Bifurcation diagram associated to a F-18 turn whose roll rate p is piloted with the control δ_a of aileron deflection

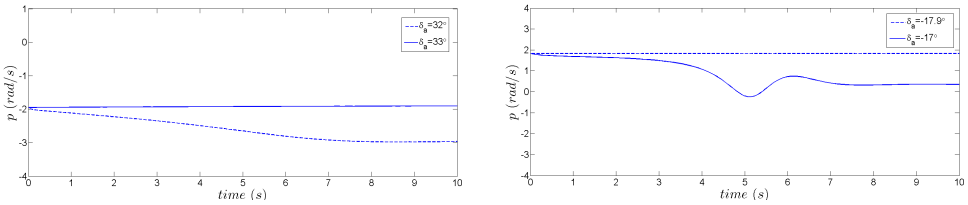

Figure 9: Time simulations for different aileron deflections ($\delta_a = 32\,\text{deg}, \delta_a = 33\,\text{deg}$ and $\delta_a = -17.9\,\text{deg}, \delta_a = -17\,\text{deg}$)

3.1. Airfoil aeroelasticity model

The classical mathematical model is based on a force equation (including lift force, plunge stiffness) and a moment equation (including pitching moment, pitch stiffness) [3]:

$$\begin{pmatrix} m_T & m_W x_\alpha b \\ m_W x_\alpha b & I_\alpha \end{pmatrix} \begin{pmatrix} \ddot{h} \\ \ddot{\alpha} \end{pmatrix} + \begin{pmatrix} c_h & 0 \\ 0 & c_\alpha \end{pmatrix} \begin{pmatrix} \dot{h} \\ \dot{\alpha} \end{pmatrix} + \begin{pmatrix} k_h(h) & 0 \\ 0 & k_\alpha(\alpha) \end{pmatrix} \begin{pmatrix} h \\ \alpha \end{pmatrix} = \begin{pmatrix} -L \\ M \end{pmatrix} \tag{5}$$

Writing the second order ordinary differential equation under the canonical form, the state vector is $X = \left\{h, \alpha, \dot{h}, \dot{\alpha}\right\}$ and the control vector is $U = \{V, \beta\}$ (variables of airspeed and flap deflection angle intervening in the calculation of lift and pitching moment).

The aeroelasticity of an airfoil may present nonlinear features. The ones which are considered here come from the pitch (torsional spring k_α) or plunge stiffness (translational spring k_h). As far as the overall behaviour is considered, apart from the classical change of equilibrium stability at the critical flutter speed, they impact the way limit cycle oscillations are created near the corresponding Hopf bifurcation point.

In order to perform the concrete analysis, the different diagrams of bifurcation theory are plotted and allow to determine the underlying dynamics and the structural changes. Generally in order to determine the Hopf bifurcation type, the algebraic expressions (normal forms) are used and allows to calculate the Lyapounov coefficient [5]. Here numerical simulations are performed so as to see the behaviours linked to the different situations e.g. periodic orbits, equilibria which are stable or unstable.

Nevertheless for the aeroelasticity problem, since the main equilibrium state value is

clearly known to be zero, the most important points consist in determining the critical flutter speed, the Hopf bifurcation type that is to say whether it is supercritical with stable limit cycles or subcritical with unstable limit cycles and potentially the enveloppe of periodic orbits. It implies respectively slowly growing oscillations or oscillations of large amplitude even before reaching the bifurcation critical speed. From the practical point of view, the last situation is quite dangerous and must be avoided [3].

3.2. Sensitivity to physical parameters

Several conclusions can be drawn concerning the sensitivity to physical parameters. The plunge stiffness seems to be favourable that is to say to imply a supercritical Hopf bifurcation. On the contrary, the pitch stiffness seems to be unfavourable in the sense that they induce a subcritical Hopf bifurcation. These statements will be illustrated in the following section.

In the model furnished in [9] and [7], the stiffness is hardened towards either plunge or pitch. The plunge stiffness comes from the spring constant for plunge degree of freedom. A nonlinear law is taken into account $k_h : h \mapsto K_h\left(1+\xi_h h^2\right)h$ with $\xi_h = 0.09$ and $\xi_h = 50$ instead of the standard linear $k_h : h \mapsto K_h h$. The Hopf bifurcation associated to $\xi_h = 0.09$ is subcritical and the one associated to $\xi_h = 50$ is supercritical as can be seen in the bifurcation diagrams (figure 10). As a consequence, the plunge stiffness hardening seems to have a nefast effect on the overall behaviour.

For the the second case study, the benchmark described in [1] is exploited for the linear part and the pitch stiffness follows the chosen nonlinear law

$$k_\alpha : \alpha \mapsto K_\alpha\left(1+10\alpha^2\right)\alpha \tag{6}$$

In figure 11, the bifurcation diagram is plotted and contains two bifurcations. There are a classical Hopf bifurcation which is supercritical and also a branch point (pitchfork bifurcation), this last one is linked to a real negative eigenvalue which becomes positive (the system remains globally unstable). The linear frame would only determine the respective flutter speed and divergence speed of the zero equilibrium. But in the nonlinear frame, the presence of stable limit cycles created at the Hopf bifurcation reduces the negative impact of the unstable equilibrium since the amplitude of the oscillations are limited. If the destabilization due to flutter is managed thanks to a feedback loop, then the presence of stable equilibria after the pitchfork bifurcation limits also the amplitudes of plunge and pitch. Thus the pitch stiffness hardening ($k_\alpha : \alpha \mapsto K_\alpha\left(1+\xi_\alpha\alpha^2\right)\alpha$ instead of $k_\alpha : \alpha \mapsto K_\alpha\alpha$) seems to have a beneficial effect.

Conclusion

The bifurcation theory allows to show and to explain some phenomena of aircraft flight dynamics and airfoil aeroelasticity. The sudden apparitions of periodic orbits and of multiple equilibria are diagnosed. The characterisation of the associated bifurcations in terms of type and control parameter values permits to assess their level of hazardousness from the practical point of view.

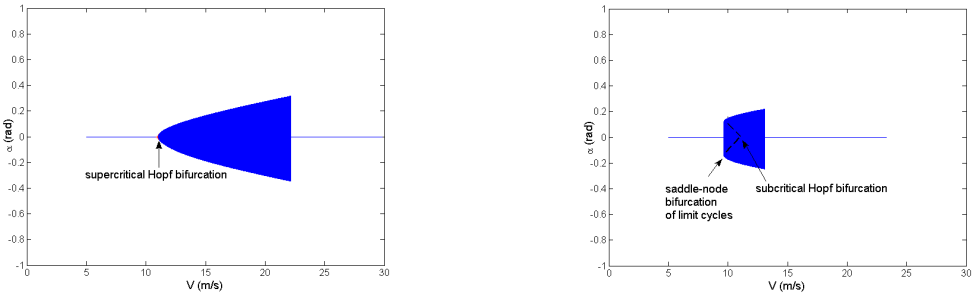

Figure 10: Bifurcation diagrams with airspeed V as control parameter presenting limit cycles and equilibria for nonlinear plunge stiffness with $\xi_h = 50$ (left) and $\xi_h = 0.09$ (right)

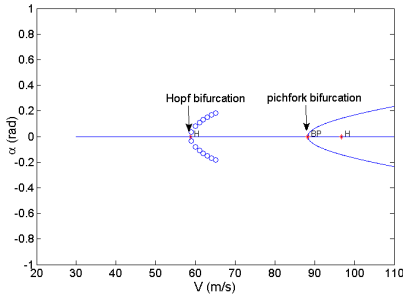

Figure 11: Bifurcation diagrams with airspeed V as control parameter presenting limit cycles and equilibria for nonlinear pitch stiffness with $\xi_\alpha = 10$

Concerning the longitudinal flight dynamics, the existence of periodic orbits and of equilibria at a nonzero bank angle present a risk for the flight safety in a situation which seems apparently completely normal. For the aircraft turns, the fold bifurcations and associated jumps reveal the effective range of the lateral control which can be used without any problem.

As far as the airfoil aeroelasticity is concerned, the hardening of the stiffness in pitch or in plunge can have a positive or a negative effect. Determining the type of the associated Hopf bifurcation that is to say supercritical or subcritical is the main feature so as to evaluate the dangerousness of the configuration and especially the sufficiency of the determination of the classical critical flutter speed.

Nomenclature

Common

U	control vector	X	state vector
L	lift (N)	M	pitching moment ($N.m$)
V	airspeed (m/s)		

	Flight dynamics
α	angle-of-attack (rad)
β	sideslip angle (rad)
δ_a	aileron deflection angle (deg)
δ_e	elevator deflection angle (deg)
δ_r	rudder deflection angle (deg)
δ_x	thrust throttle (%)
γ	flight-path angle (rad)
ϕ	bank angle (rad)
θ	pitch angle (rad)
ψ	heading angle (rad)
x, y	aircraft position coordinates (m)
h	altitude (m)
p	roll rate (rad/s)
q	pitch rate (rad/s)
r	yaw rate (rad/s)

	Aeroelasticity
m_T	total mass of the wing (kg)
m_W	wing mass alone (kg)
I_α	mass moment of inertia about the elastic axis
b	half chord length (m)
x_α	nondimensionalized distance between the center of mass and the elastic axis
h	plunge (m)
α	angle-of-attack/pitch angle (rad)
β	flap deflection angle (rad)
ρ	air density (kg/m^3)
c_h	plunge structural damping coefficient
c_α	pitch structural damping coefficient
k_h	plunge stiffness
k_α	pitch stiffness

References

[1] Axisa, F. *Vibrations sous écoulements*. Hermes, 2001.

[2] Dhooge, A., Govaerts, W., and Kuznetsov, Y. A. Matcont: A matlab package for numerical bifurcation analysis of odes. *ACM Trans. Math. Softw. 29*, 2 (2003), 141–164.

[3] Dimitriadis, G. *Introduction to nonlinear Aeroelasticity*. John Wiley & Sons Ltd, 2017.

[4] Fan, Y., Lutze, F. H., and Cliff, E. M. Time-optimal lateral maneuvers of an aircraft. *Journal of Guidance, Control, and Dynamics 18*, 5 (1995), 1106–1111.

[5] Guckenheimer, J., and Holmes, P. *Nonlinear Oscillations, Dynamical Systems and Bifurcations of Vector Fields*, vol. 42 of *Applied Mathematical Sciences*. Springer, 2002.

[6] Härkegård, O. Backstepping and control allocation with applications to flight control. Master's thesis, Linköping University, 2003.

[7] O'Neil, T., and Strganac, T. W. Aeroelastic response of rigid wing supported by nonlinear springs. *Journal of Aircraft 35*, 4 (1998).

[8] Sinha, N. K., and Ananthkrishnan, N. *Elementary Flight Dynamics with an Introduction to Bifurcation and Continuation Methods*. Taylor & Francis Group, 2017.

[9] Strganac, T. W., Ko, J., Thompson, D. E., and Kurdila, A. J. Identification and control of limit cycle oscillations in aeroelastic systems. *Journal of Guidance, Control, and Dynamics 23*, 6 (2000).

S. Kolb
CReA, French Air Force Research Centre
BA 701, 13661 Salon Air, France
sebastien.kolb@ecole-air.fr